



Characterization of the skill of the CORDEX-Africa regional climate models to simulate regional climate setting in the East African Transboundary Omo Gibe River Basin, Ethiopia

Yonas Mathewos^{a,*}, Brook Abate^b, Mulugeta Dadi^a

^a Faculty of Biosystems and Water Resources Engineering, Institute of Technology, Hawassa University, Ethiopia

^b College of Architecture and Civil Engineering, Addis Ababa Science and Technology University, Ethiopia

ARTICLE INFO

Keywords:

CORDEX-Africa
Climatic setting
Multi-model ensemble
RCMs
Skill

ABSTRACT

Regional climate models (RCMs) that produce good outputs in one region or for specific variables may underperform for others. Thereby, assessing the performance of various model simulations and their corresponding mean ensemble is critical in identifying the most suitable models. In this regard, a study was conducted to evaluate the performance of ten RCMs against observations from multiple ground-based stations in the East African Transboundary Omo Gibe River Basin, Ethiopia, during the baseline period of 1986–2005. The study evaluated the models' ability to replicate various aspects of climatic variables and their corresponding statistical indicators. The results confirmed that RCMs have varying abilities to reproduce climatic conditions across the basin. The ensembles and RACMO22T (EC-EARTH) were better at replicating the average annual precipitation distribution. Meanwhile, the CCLM4-8-17 (MPI) together with the ensembles better captured the measured precipitation annually, despite the discrepancies in the actual magnitudes. All RCMs were able to simulate the seasonal precipitation patterns effectively, with RACMO22T (EC-EARTH), CCLM4-8-17 (CNRM), RCA4 (CNRM), CCLM4-8-17 (MPI), and REMO2009 (MPI) models captured superior, excluding the maximum value. Interannual and seasonal rainfall pattern variations were more significant than variations in air temperature. Additionally, a better correlation was observed between actual and simulated precipitation at multiple separate monitoring places. The RCA4 (MPI) and CCLM4-8-17 (MPI) demonstrated reasonable minimum and maximum temperatures. The RCA4 (MIROC5) model was more effective in reproducing extreme precipitation events. However, all RCMs and their ensembles tended to overestimate the return periods of these events. In general, the research highlights the importance of selecting reliable RCMs that better replicate observed climatic settings and employing the ensemble mean of top-performing models following systematic bias adjustment for a specific application.

1. Introduction

Climate change has become a pressing issue worldwide, affecting every region, and ecosystem. The increase in atmospheric greenhouse gases is a significant driving force behind the changing climate patterns observed across the world [1]. Human activities such as industrial development and forest destruction have contributed greatly to the rise in atmospheric CO₂ levels, which in turn

* Corresponding author.

E-mail address: yonasmathewos4@gmail.com (Y. Mathewos).

<https://doi.org/10.1016/j.heliyon.2023.e20379>

Received 21 June 2023; Received in revised form 20 September 2023; Accepted 20 September 2023

Available online 24 September 2023

2405-8440/© 2023 The Authors. Published by Elsevier Ltd. This is an open access article under the CC BY-NC-ND license (<http://creativecommons.org/licenses/by-nc-nd/4.0/>).

amplifies the effects of climate change [2]. This has led to alterations in precipitation patterns, with extreme events becoming more frequent in many regions globally. Developing nations were significantly susceptible to climatic change owing to their low adaptive capacity and reliance on rain-fed agriculture [3–7]. In Africa, these changes are adversely affecting human health, agriculture, biodiversity, and infrastructure [3–7]. The outcomes of climatic variability are most rigorous in vulnerable communities, particularly in Sub-Saharan countries like Ethiopia [8]. Moreover, the changing climate, with altered rainfall patterns and intensifying temperatures, is worsening challenges like food insecurity, water scarcity, and economic development. The situation is further aggravated by factors like agricultural growth, fast population increase, and the devastating impacts of extreme weather events such as floods and droughts [9].

The country Ethiopia's, agricultural sector serves as the backbone of the economy and provides food for 85% of the community [10, 11]. Approximately 90% of agrarian output depends on rainwater, which coupled with fluctuations in air temperature could significantly affect the sector [12]. Ethiopia's high susceptibility to climate instability is due to its reliance on precipitation-driven agriculture, untapped water potential, and insufficient management of river basins [13]. As a result, it is frequently affected by starvation and numerous socio-economic catastrophes [14,15]. Thus, addressing these impacts is crucial for guaranteeing the long-term viability of Ethiopia's freshwater systems, food security, and economic stability.

Currently, African countries lack nation-specific tools to examine the climate impact in the targeted region [4]. To effectively address the existing gaps in envisaging climate change at the localized expanse and conduct detailed impact assessments, applying suitable RCMs is essential [16]. To that end, analyzing historical climate data through observational records is critical to predict the models' ability and assess the potential consequences of future climate change from various viewpoints [17]. Despite their relevance in predicting overall climate change trends, GCMs often suffer from coarse spatial resolution, making them less effective for local-scale projections [4,5,18]. This issue also affects GCMs' capacity to accurately depict extreme hydrological events [19,20]. As a result, downscaling GCM outputs to higher regional-scale resolution is necessary for obtaining more suitable spatiotemporal information in future climate projections.

Over the past decades, RCMs have emerged as a powerful tool for simulating regional climate and providing high-resolution climate scenarios for environmental impact studies. Recently, the RCMs can have spatial resolutions ranging from $0.44^\circ \times 0.44^\circ$ to less than $0.044^\circ \times 0.044^\circ$ [21]. This enhanced resolution allows RCMs to better represent regional features and small-scale processes, resulting in a more accurate simulation of regional climates compared to their driving data [9,22]. However, in regions dominated by large-scale climatic processes, this may not always be the case [7]. Thus, the added value of high-resolution RCMs is highly dependent on the specific region, variable, and context being analyzed. Precipitation and air temperature are critical climatic variables driving the regional hydrological cycle and ecosystems, as well as impacting human society and the regional economy. Numerous explorations have confirmed that RCMs are capable of generating highly accurate yearly and seasonal replications of temperature and rainfall [20, 23]. As a result, RCMs have become a favored tool for analyzing the patterns and frequency of severe rainfall events. The research performed [7] found that RCMs replicated reasonably in modeling air temperature, but their ability to simulate precipitation patterns was considerably less, highlighting the inconsistent performance of these models. Likewise [24], discovered varying RCM performance across a large area of Tanzania using observed station data. Ensemble RCMs in Africa were shown to align better with observed data than individual RCMs [25]. Using ensembles from various RCM outputs did not consistently guarantee the closest correspondence between observed and modeled climate variables. Therefore, accurate spatial representations of these variables are essential for understanding regional climate processes and predicting future climate change impacts.

In Ethiopia, research has indicated that RCMs exhibit a noticeable bias at higher elevations, but they demonstrate accurate results when applied to areas situated at lower altitudes [4,5,20]. However, studies have concentrated on understanding the susceptibility to climate change and implementing potential mitigation strategies by employing individual simulations [26,27]. Furthermore [5,25] confirmed that not all RCMs demonstrate the same level of effectiveness in producing specific regions. The varying effectiveness of RCMs in replicating diverse expanses and timeframes highlights the importance of assessing the susceptibility of a particular area by utilizing multiple RCMs, to determine the most suitable RCMs for a localized study area. The OGRB contains multiple cascaded dams for significant hydroelectric power generation and agriculture, however, the basin frequently faces the problem of extreme hydrological events, such as droughts, floods, and other extreme weather events associated to dynamic natural and anthropogenic issues. That could significantly impact power production, crop yields, and food security in the region. However, previous studies in the basin have primarily focused on assessing the effects of climate change on hydrological processes [28–30], stream flow simulation [31–34], drought characteristics analysis, and groundwater recharge estimation at small catchment levels [35,36]. However, there is a lack of specific studies that have exclusively evaluated and identified suitable RCMs for assessing climate trends and their future impacts, even though the basin is vulnerable to the impacts of climate change of unprecedented magnitude. Such studies are essential for identifying high-resolution RCMs that perform better in reproducing observed precipitation and temperature patterns during the reference period. Moreover, the current study can inform the application of these models in simulating and predicting the future impacts of climate change on water resources and agriculture in the region.

This study focuses on evaluating the skill of ten widely used CORDEX-Africa Regional climate models in simulating the regional climatic settings of the East African Transboundary Omo Gibe River Basin in Ethiopia. The goal is to ensure reliable future climate projections and inform decision-making on water resource management and adaptation strategies in the region. By comparing observational data with model outputs, the study thoroughly assesses the models' performance in representing various climatic variables like temperature and precipitation. The findings provide a basis for refining the projections of climate change impacts on the hydrology and water resources of the region. The study is structured into several sections, including an abstract, introduction, materials and methods, results and discussion, conclusion, and references.

2. Study area

The Omo Gibe River Basin (OGRB) covers a total area of approximately 79000 km². The OGRB stands as a cornerstone among the nation's crucial river basins and contains invaluable resources such as widespread irrigation projects and hydroelectric power generation stations. The Omo River flows for about 1000 km from its source in the Ethiopian highlands and traverses southwestern Ethiopia, ending its flows into Lake Turkana situated in Kenya. The basin is further characterized by diverse climatic conditions, ranging from humid highland regions to arid lowlands [34,37,38].

3. Material

3.1. Regional climate models and their deriving datasets

RCMs and GCMs have been extensively used in climate research. The CORDEX program used RCMs to downscale the outputs of GCMs and provide regional climate projections for different parts of the world [39]. These baseline GCM replications provided initial boundary conditions and were based on observed atmospheric, oceanic, terrestrial, and sea surface temperatures, as well as natural and human-induced CO₂ and aerosol concentrations [20,40]. Each RCM considered both the baseline scenario replication and initial ensemble element (r1) for analysis. The simulation outcomes were derived from the CORDEX initiatives for the African region, with a spatial fineness of approximately 25 km × 25 km. In the CORDEX Africa domains, specific models including CanRCM4, RACMO22T, REMO2009, RCA4, and CCLM4-8-17 were employed to regionalize GCMs. The utilization and characteristics of these models, in conjunction with their respective features, are detailed in Table 1. The models were chosen based on factors like data availability for different combinations of RCM, GCM, representative concentration pathways (RCPs), spatial resolution, their usage in African watersheds, computational efficiency, the inclusion of established and new models, and the existence of the first ensemble member (r1). For consistency, a uniform analysis period of 1986–2005 was employed across all regional climate models, even though the recreated reference data covered the range of 1950–2005. This period of 20 years was deemed appropriate for evaluating the performance of the selected models, considering the limited availability of observed data. Other studies conducted by Refs. [41,42] reinforced that this period was adequate to assess the performance of the individual models. However, the selection criteria also took into account the projected data for future scenarios spanning from the periods of 2006–2100, for future climate change impact assessments in the region. Various research studies have tested and corroborated the efficacy of these models in replicating precipitation patterns and temperature fluctuations across the African continent [4,5,20,23]. In OGRB, the skill of these RCMs has not been fully assessed, except for studies of [4] that focused on the Jimma and upper Gilgel Gibe expanses. The precipitation and air temperature information from RCMs were acquired through the Earth System Grid Federation's public access portal, available at: <https://esgf-node.llnl.gov/search/esgf-llnl/>, and extracted using coordinates of the individual stations in the ArcGIS environment.

3.2. Monitored meteorological information

The absence of prolonged recorded climatic information in Ethiopia hampers the understanding of crucial areas in climate model representations that require significant enhancement. Many meteorological monitoring systems were set up across the country in response to the drought that occurred in the mid-1980s. The assessment of the diverse model mimicked outcome necessitates the use of measured data for comparison. Despite significant differences between the observed and satellite data, numerous researchers have employed satellite-derived information to validate RCM outcomes. Climatological analysis, derived from ground-based observations has precisely replicated and facilitates an exhaustive assessment of the simulated precipitation patterns on a localized scale [49]. Several studies in Ethiopia demonstrated the importance of using observed meteorological data to validate the performance of RCMs in simulating climate conditions [4,5,19,26]. Hence, daily time step temperature and precipitation information was procured from the

Table 1

Represents RCMs and their deriving sources utilized.

Description of the RCMs	Driving sources	RCMs	Reference
Koninklijk Nederlands Meteorologisch Institute (KNMI), Regional atmospheric climate model version 2.2, Netherlands	ICHEC-EC-EARTH	KNMI-RACMO22T	[43]
Sveriges Meteorologiska och Hydrologiska Institute (SMHI), The Rossby Centre Regional Climate model, Sweden	CNRM-CERFACS-CNRM-CM5 MPI-M-MPI-ESM-LR MOHC-HadGEM2-ES MIROC-MIROC5	SMHI-RCA4	[44]
COnsortium for Small-scale MOdeling (COSMO) Climate Limited Area modelling Community (CLMcom), USA	CNRM-CERFACS-CNRM-CM5 MOHC-HadGEM2-ES MPI-M-MPI-ESM-LR MPI-M-MPI-ESM-LR	CLMcom-CCLM4-8-17	[45]
Max Planck Institute for Meteorology-Climate Service centre (MPI-CSC), Regional Model, Germany	MPI-M-MPI-ESM-LR	MPI-CSC-REMO2009	[46]
The Canadian Centre for Climate Modeling and Analysis second generation Earth System Model, Canadian Regional Climate Model version 4	CCCma-CanESM2	CCCma-CanRCM4	[47,48]

Ethiopian National Meteorological Service Agency, which considered 20 monitoring site records from 1986 to 2005, as demonstrated in Fig. 1. To choose the ground-based stations the spatial distribution of the stations, altitude, quality and length of the station records, and availability of data from different seasons and climatic zones were considered, to ensure the representativeness of the region being modeled.

The climatological investigation typically needs complete datasets with no gaps or missing records, as missing data can disrupt the continuity of records due to observer absence or instrument failure. Thus, determining and filling in the missed information is crucial before employing it for water balance scrutiny, which is accomplished through a process known as data imputation. Consequently, meteorological stations with precipitation and temperature records, as described in Table 1, were utilized for basin analysis. All stations portrayed a low 6% of missing data for the entire period. The missing information was replaced by applying XLSTAT 2018 before analysis, which has been employed to scrutinize the links between multiple parameters simultaneously [50]. The assessment primarily depends on historical climate data, encompassing observed variables like temperature and precipitation. The fundamental assumption underlying this study is that the historical data available accurately reflect the past climate conditions within the study area. Furthermore, the ground-based observational data obtained from meteorological stations, which were used to validate the RCM simulations, are assumed to be representative of the actual climate conditions in OGRB. According to a study carried out by Refs. [51, 52], it is necessary to verify the essential assumptions of hydrological data, such as randomness, independence, homogeneity, and stationarity, before proceeding with time series analysis. Failure to meet these assumptions may lead to uncertain results. This study examined data from all monitoring sites and confirmed that the basic assumptions were met, indicating that the data can be used for further analysis. A homogeneity test was assessed through the application of the Standard Normal Homogeneity Test (SNHT) in XLSTAT, which aids in pinpointing discrepancies within a chronological precipitation dataset by juxtaposing the average values of the initial k years with those from the last $n-k$ years of the record [53,54]. Discrepancies, like the minimum temperature surpassing the maximum temperature and negative rainfall, data from adjacent stations were utilized for accurate corrections. Anomalies deviating significantly beyond the mean of \pm four times the standard deviation were identified as outliers and rectified by averaging the corresponding values obtained from days preceding and succeeding the aberrant day, following WMO guidelines [5]. A thorough examination of the collected data ascertained its homogeneity, affirming that all stations under consideration contributed consistent and coherent information.

4. Methods

Two skill assessment metrics were employed to determine the effectiveness of RCMs in simulating the climate of the entire region being analyzed. The initial metric examined the skill of the RCMs in reproducing the climatic settings of rainfall and air temperature as well as the characteristics of precipitation events. This involved comparing the RCMs' outputs with observed data, considering average values of yearly and seasonal rainfall, monthly rainfall patterns, distribution and occurrence of rainfall events, and return periods. The second assessment metric utilized statistical indicators such as BIAS, Root Mean Squared Error, and Correlation Coefficient (Correl) to quantitatively measure the relationship between the areal-averaged precipitation data from the RCMs and the observed data.

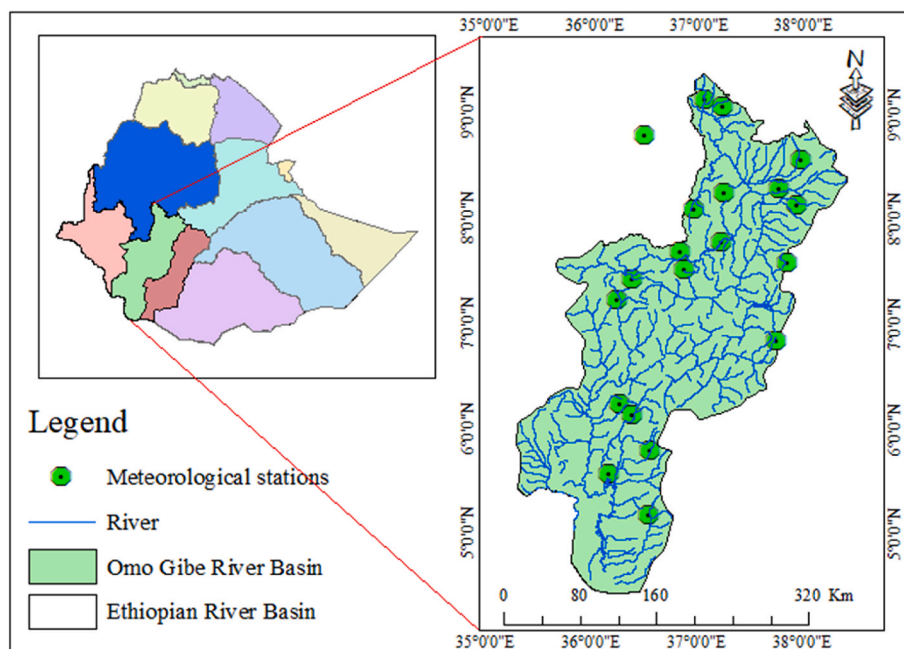


Fig. 1. Location map of the OGRB with climatic parameter monitoring sites.

4.1. Observed and RCMs performance assessment metrics

The corroboration of RCMs’ ability to replicate observational climatic conditions such as precipitation and temperature for the baseline timeframe has not been exclusively applied for their possible application in future climate change impact studies in the area. To better understand the systematic and dynamic behavior of these models, the mimicked and measured output data were plotted on the same coordinate system for visual comparison. However, not all models demonstrated equal proficiency in simulating climate data, as various factors, including land characteristics, influenced their performance [4,5]. To assess the capability of different models mimicking mean yearly precipitation and temperature, various statistical methods, such as the PBIAS, the Root Means Square Error (RMSE), and the Pearson correlation coefficient (r) were employed. The effectiveness of these evaluation metrics has been elucidated and reinforced by numerous analyses [4,5,41,55–57].

The process of assessing the disparities in percentage terms between the outcomes derived from RCMs and the observations was conducted distinctively for both precipitation and temperature variables. Negative figures signify an underestimation, while positive figures represent an overestimation in mimicked. Those figures nearest to zero indicate the least systematic divergence and most accurate estimation from climate prediction. The following empirical formulas in equation (1) were employed to analyze the bias of precipitation and temperature for the ten chosen RCMs and their corresponding average ensembles across OGRB.

$$BIAS = \frac{1}{n} \sum_{i=1}^n (S_i - O_i) \tag{1}$$

The RMSE represents the total deviation in climate model simulations for predicting climatic conditions, and it calculates the difference between the outputs of RCMs and station observations as shown in equation (2). The RMSE has a similar unit as the measured factors, allowing for easy elucidation, with a value close to zero indicating high model accuracy.

$$RMSE = \sqrt{\frac{1}{n} \sum_{i=1}^n (S_i - O_i)^2} \tag{2}$$

The correlation coefficient (r) and the coefficient of determination (r²) are frequently utilized methods in various research to analyze the relationship between two variables. For instance, Pearson’s correlation coefficient assesses the linear association and goodness of fit between parameters such as RCMs and observed [58–60]. This coefficient evaluates how well climate indices derived from climate simulations replicate observation. Daily inputs for the variables were utilized for calculating climate index values with the yearly time step. Pearson’s correlation coefficient is employed, with its mathematical formula provided in equation (3). Its value ranges from 1 to –1, where a positive value signifies a strong positive association, a negative value denotes a strong negative association, and a zero value implies a weak or nonexistent association.

$$r = \frac{\sum_{i=1}^n (S_i - S_m) (O_i - O_m)}{\sqrt{\sum_{i=1}^n (S_i - S_m)^2} \sqrt{\sum_{i=1}^n (O_i - O_m)^2}} \tag{3}$$

in this context, S represents the mimicked value from the model, while O denotes the measured value of the climate parameters. The index i corresponds to the mimicked and measured pairs, n signifies the total number of pairs, and m refers to the average.

Generally, the lower the bias and RMSE, the better the model performance, and vice versa. The correlation coefficient can range from –1 (perfect negative correlation) to 1 (perfect positive correlation) between RCMs and observed climate variables. Often, no sole metrics can consistently determine the superior model, so BIAS, RMSE, and r are applied together. It’s possible to have an acceptable r deviation from 1, but not an acceptable common value for BIAS and RMSE. In this sense, there’s no agreed-upon limit, but lower BIAS and RMSE values indicate more accurate model predictions. Nonetheless, excessively low values might result in overfitting.

4.2. Precipitation and air temperature variability

The coefficient of variability (CV) was employed to examine variability in precipitation data on both seasonal and yearly scales as shown in equation (4). Data with a higher CV value is more variable, with figures under 20 signifying slight changeability, those between 20 and 30 signifying moderate erraticism, and those over 30 demonstrating higher variations [61].

$$CV = 100 * \frac{\sigma_R}{\bar{R}} \tag{4}$$

The symbol with a bar represents the arithmetic mean employed throughout the analytical timeframe (1986–2005), with the analysis period (N) being 20 years; R signifies the mean annual precipitation in the basin for a specific year (t); σ pertains to the standard deviation of the simulated or measured data. R without a subscript means that the statistics are computed distinctly for simulated or observed datasets. The CV calculated for measured and simulated precipitation by the RCMs evaluates how well the models capture and represent the precipitation variability through the network’s stations.

To demonstrate the consistency of model simulations, RCM simulations should account for the variation in yearly precipitation from the long-term average. Therefore, the precipitation anomaly (RA) of the mimicked and measured, defined for the station data in a

given year (t), is given as follows in equation (5).

$$RA = \frac{R_i - \bar{R}}{\bar{\sigma}} \quad (5)$$

The parameters within the aforementioned formula have been distinctly identified. This particular formula is individually employed for both gauge-based precipitation measurements and RCM precipitation datasets. Furthermore, this study employs a second evaluation criterion, focusing on assessing the annual patterns of rainfall and temperature. It investigates how well RCMs replicate the seasonal patterns of precipitation and temperature. Furthermore, the third evaluation criteria analyzes the single models and ensembles' mean skill to replicate the inter-annual changeability of rainfall and temperature in the basin. To achieve this, the study scrutinizes the time-dependent data of spatial mean rainfall and temperature anomalies from June to September (JJAS) and March to May (MAM).

4.3. Spatial assessment of measured and RCMs rainfall distribution

Spatial analysis of observed and RCM precipitation is crucial to understanding the spatial distribution, variability, and changes in precipitation patterns. Recent studies have applied various techniques to analyze the spatial pattern of observed and RCM precipitation and have provided valuable insights into their distribution, variability, and factors influencing them. For example, studies conducted by Ref. [62] have explored different geostatistical and deterministic approaches to spatial interpolation and revealed the performance could vary based on factors such as the density of weather stations. In particular, the studies confirmed that ordinary Kriging and inverse distance weighting (IDW) methods tend to produce better results and smaller root mean square error (RSME) values than other methods. Likewise [5], examined the performance of various prediction systems, and demonstrated that the Inverse Distance Weighting (IDW) technique yielded superior results. In this investigation, a rough comparison of IDW, kriging, and spline methods revealed that ordinary kriging estimations were more accurate when using a larger number of stations. Using ArcGIS 10.4.1, the RCM simulation data were extracted from four grid points surrounding the observation station, and the mimicked values were interpolated to the measured utilizing ordinary kriging. These techniques involved calculating the weights for each interpolated point, taking into account the spatial configuration of the entire array of sampled points at the given interpolated location. The weights were then derived from the variogram, reflecting the data's spatial structure, and subsequently applied to the sampled points, which can be expressed mathematically as follows in equation (6):

$$\hat{Z}(X_0) = \sum_{i=1}^N \lambda_i Z(X_i) \quad (6)$$

in the kriging interpolation technique, the estimated outcome for the anticipated point (z-hat) at a specific location (x-naught) is computed by summing the product of each observed point's value (x) at position i with its respective exclusive weightage (lambda) for that specific location i. These individual weightage factors are ascertained using the covariance framework of the approximated variogram and may exhibit minor variations based on the kriging technique implemented.

5. Results and discussion

5.1. Annual precipitation pattern

Precipitation in Ethiopia, specifically in the OGRB, plays a crucial role in development activities as the region relies heavily on rainfall-based agriculture. Thus, the accurate appraisal of model simulations on a localized level becomes a critical cornerstone for driving meaningful and influential climate impact examination [9]. The RCMs outcomes and conforming averaged ensembles were assessed by examining their capability in simulating measured yearly climate, inter-annual fluctuations, seasonal variations in precipitation and air temperature, as well as specific precipitation attributes within the region. The findings in the region portrayed RCMs outputs overestimated the average annual precipitation, exclusively CanRCM4 (CanESM2), RCA4 (MIROC5), and RCA4 (MPI), some others like CCLM4-8-17 (HadGEM2), CCLM4-8-17 (MPI), and REMO2009 (MPI) took a distinct approach by underestimating this critical parameter. The overall relative bias among all RCMs results was identified to be below 20%, signifying a tolerable threshold for precipitation replication. CCLM4-8-17 (HadGEM2) demonstrated the highest relative bias of 11.95 at the Sawla station, while CCLM4-8-17 (CNRM) showed the lowest 0.02 for the Dimeka station, as detailed in Table S1. Interestingly, the climate models overestimated precipitation in areas such as Emdibir, Gedo, and Gojeb stations, while they underestimated it in Sawla, Wolaita Sodo, and Keyafer at the lower part of the basin.

Regarding the RMSE metric, most RCMs demonstrated superior performance in capturing annual precipitation patterns, apart from some stations located in the upper and lower parts of the basin, including Emdibir, Gedo, and Hossana when applying the RCA4 RCM from all groups, and Sawla, Wolaita-Soda, and Keyafer when employing all RCMs. The maximum RMSE of 12.43 was noted in the Sawla CCLM4-8-17 (HadGEM2) model, whereas the Assendabo CCLM4-8-17 (HadGEM2) model exhibited a minimum RMSE of 0.52. Systematic errors were found at the Assendabo and Woliso stations, with smaller errors occurring when using ensembles at most stations instead of individual RCMs. Considering Pearson's correlation coefficient (r), negative correlations were found between simulated annual mean precipitation and observational data for Baco, Bonga, and Wolaita Sodo stations using all regional climate models, excluding RACMO22T (EC-EARTH) at Wolaita Sodo, which showed a positive correlation. The highest positive and negative r

values were 0.88 at Limu Genet using CCLM4-8-17 (CNRM) and -0.85 at Wolaita Sodo using CanRCM4 (CanESM2), respectively. The statistical indicators of spatially averaged annual rainfall simulations are presented in Table S1.

5.2. Annual mean temperature

5.2.1. Average annual maximum temperature

Skill most of the RCMs in simulating the temperature cycle was quite remarkable, but the RCA4 (HadGEM2) and CCLM4-8-17 (HadGEM2) unfortunately, failed to reproduce the pattern of the highest yearly average air temperatures of the region. Most models provided low estimations for the highest average annual air temperature in the region, excluding REMO2009 (MPI), which provided an overestimation. The RACMO22T (EC-EARTH) and CCLM4-8-17 (CNRM) showed the smallest maximum average yearly air temperature compared to the other RCMs studied. Observed temperature bias varied across different stations, with the lowest bias of $0.02\text{ }^{\circ}\text{C}$ found at Dimeka and Bako using CCLM4-8-17 (CNRM) and CCLM4-8-17 (HadGEM2) RCMs, and the highest bias of $11.95\text{ }^{\circ}\text{C}$ recorded at Sawla using the CCLM4-8-17 (HadGEM2) model. The models demonstrated a strong negative bias at Sawla, Wolaita Sodo, and Keyafer monitoring sites, demonstrating a considerable discrepancy in these locations. Additionally, the RMSE value was high at these stations, implying that the model's representation of the actual measurement was poor. A negative coherence was found in the actual and modeled yearly average maximum temperatures by all models at Bongo and Bako, excluding RACMO22T (EC-EARTH) at Wolaita Sodo. However, a majority of the stations demonstrated a positive relationship in simulating the maximal yearly average air temperature, as shown in Table S2.

5.2.2. Minimum mean annual temperature

The ability of nearly all RCMs to capturing the lowest yearly average air temperature at various stations, such as Emdibir, Asendabo, Jimma, and others, was quite good. However, the models were highly biased at locations like Wolaita-Soda, Gojeb, Woliso, and a few others. The RCA4 (MPI) and CCLM4-8-17 (MPI) models demonstrated reasonable skill compared to other individual RCMs at the majority of weather stations under evaluation. At the Wolaita Sodo station, the greatest bias and RMSE values were recorded, with $18.44\text{ }^{\circ}\text{C}$ and 18.45 for RCA4 (HadGEM2), and $18.24\text{ }^{\circ}\text{C}$ and 18.25 for CCLM4-8-17 (HadGEM2) respectively, indicating significant discrepancies in observed data. In almost all models, including the CCLM4-8-17 (HadGEM2) and CCLM4-8-17 (MPI), RCMs tended to overestimate the lowest yearly mean air temperature when related to the actual measurements. Despite most simulation results positively correlating with observational data, the Wolaita Sodo station exhibited a negative correlation between simulated and

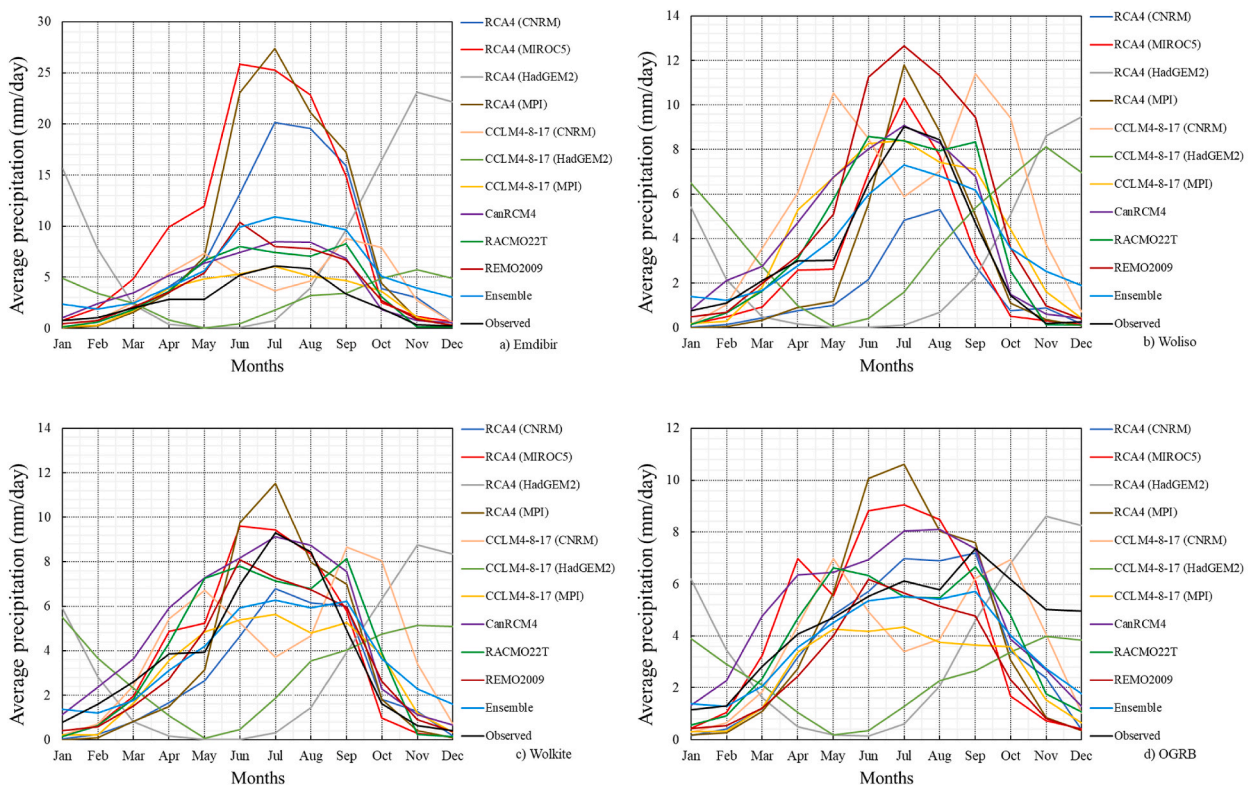


Fig. 2. The average monthly precipitation pattern for the 10 RCMs, the multi-model ensemble (a–c), and the observed data for some selected stations and the entire OGRB (d).

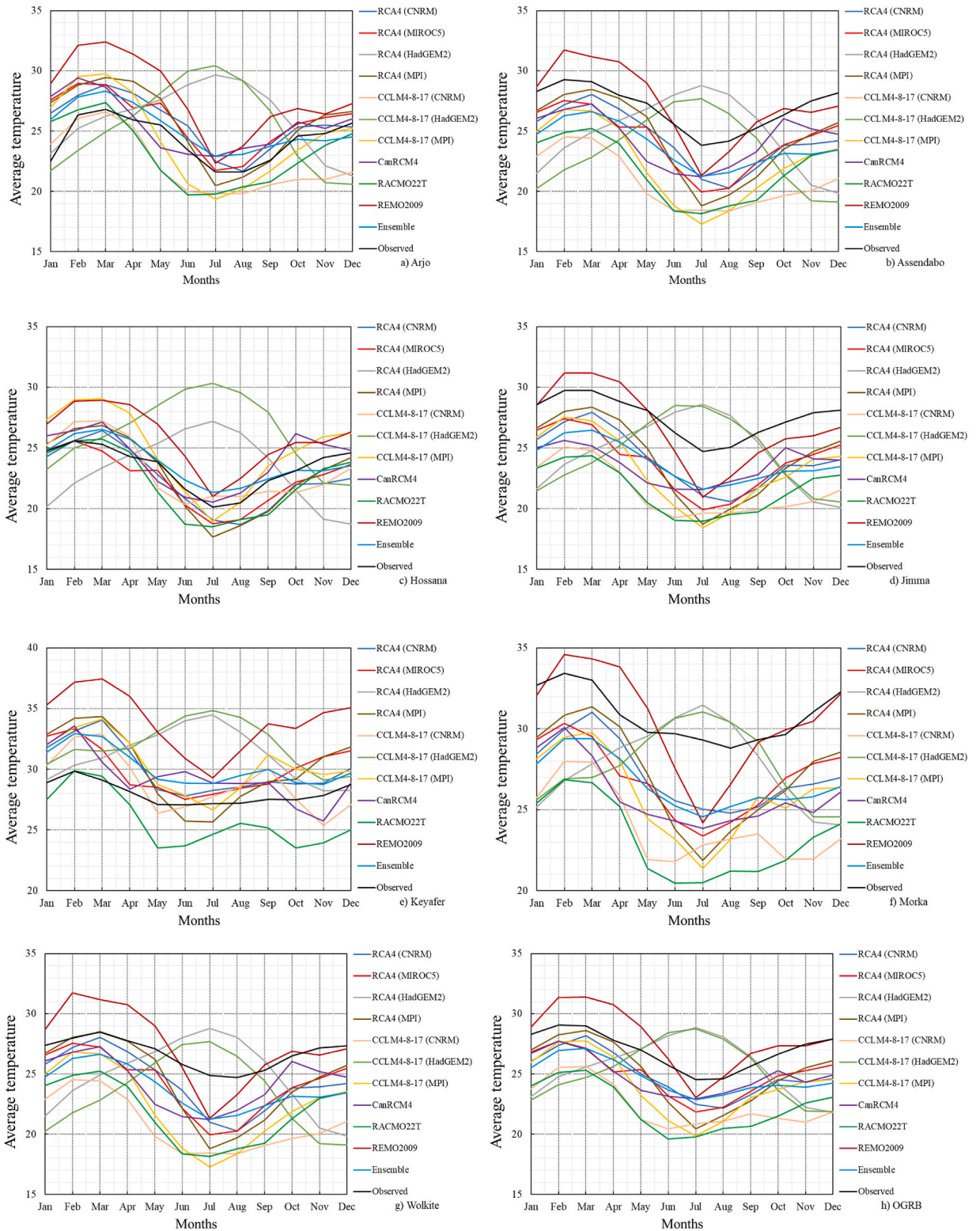


Fig. 3. Average monthly pattern of maximum air temperature for the 10 RCMs, multi-model ensemble (a–g), and observed data for the selected stations and the entire OGRB (h).

observed values (Table S3).

5.3. Average monthly climate variable pattern

5.3.1. Average monthly precipitation pattern

In the OGRB, the climatic regime is characterized by a monomodal pattern with the main rainy months occurring in JJAS, as shown in Fig. 2. The area experiences two main rainy periods, with Belg providing moderate showers from March to May, while Kiremt brings more substantial rainfall in JJAS. Between November and February, the area undergoes a dry season known as 'Bega,' which is characterized by low rainfall. In the upper areas of the OGRB, most of the model output successfully captured the observed main rainfall season during the months of JJAS, with the maximum precipitation happening in July. However, the REMO2009 (MPI) model's peak was shifted to June. In contrast, models CCLM4-8-17 (CNRM), RCA4 (MIROC5), and RACMO22T (EC-EARTH) exhibited a common error by simulating a double peak from April to September in the upper reaches, while the observed data reproduced only a single maximum in July. The RCA4 (HadGEM2) and CCLM4-8-17 (HadGEM2) models exhibited discrepancies in their precipitation replications, leading to an overestimation in drier months and an underestimation in wet months, resulting in the smallest precipitation values during wet months compared with other RCMs. Except for RCA4 (HadGEM2), the RCA4 family of models displayed significant interannual fluctuations, predicting the highest rainfall during the wet months and reduced rainfall during the dry months, particularly in the case of RCA4 (MPI). All RCMs demonstrated enhanced performance in capturing rainfall during dry months compared to wet months, excluding RCA4 (HadGEM2) and CCLM4-8-17 (HadGEM2), which failed to reproduce the intensity and distribution of precipitation across the basin. Fig. 2(a–d), and Figure S1 (a–q) depict the average monthly rainfall patterns observed at various stations, along with the outcomes from ten RCMs, the ensemble mean, and the mean monthly rainfall pattern within the basin. It was found that in the central and lower parts of the basin, two significant precipitation maximal occurred, one in the period of March–May (MAM) and another between August–November (ASON). In these regions, the majority of climate models successfully reproduced the highest rainfall between March–June, with the peak month being May; however, the CanRCM4 (CanESM2), RCA4 (MIROC5) models, and actual data indicate that the maximum precipitation in April. Likewise, the REMO2009 (MPI) and RCA4 (MIROC5) models exhibit maximum rainfall during September, which is in contrast to the majority of other models that pinpoint October as the month with the highest precipitation. Generally, RCMs displayed superior in replicating rainfall amounts during drier months against the wettest ones, excluding RCA4 (HadGEM2) and CCLM4-8-17 (HadGEM2) models. In the wettest period, a majority of the models tended to over-predict precipitation, while RCA4 (HadGEM2), CCLM4-8-17 (CNRM), CCLM4-8-17 (HadGEM2), and CCLM4-8-17 (MPI) models revealed underestimations in their replications.

In general, understanding the practical implications of both overestimated and underestimated precipitation in various parts of the basin is very crucial, because agriculture in the area heavily depends on rainfall. Overestimated precipitation can cause waterlogging, soil erosion, and reduced crop yields, leading to decreased agricultural productivity and economic vulnerability for farmers in affected areas. However, a study by Refs. [63,64] showed that overestimation of precipitation could lead to crop surpluses and subsequent financial losses due to market price drops. In contrast, in areas where precipitation was underestimated, may result in insufficient yields, food shortages, and increased economic vulnerability. In addition, a study by Ref. [65] found that overestimation of precipitation could lead to overuse of water resources, depleting groundwater and surface water resources and exacerbating water stress in the region. Conversely, underestimation of precipitation can lead to underuse of water resources, decreased agricultural productivity, and increased economic vulnerability. Therefore, to address these practical implications of overestimated or underestimated precipitation, improved climate monitoring and forecasting tools were needed that provide more accurate and reliable information on precipitation patterns and variability.

5.3.2. Average monthly highest and lowest air temperature patterns

a. Average monthly highest temperature pattern

In all months, most model outputs did not accurately capture the average maximum air temperature, except REMO2009 (MPI), which provided a more accurate simulation. RACMO22T (EC-EARTH) and CCLM4-8-17 (CNRM) performed poorly in modeling the highest air temperatures, whereas REMO2009 (MPI) exhibited a better depiction of the temperature cycle across the region, as shown in Fig. 3. In addition, RCMs predicted the highest monthly air temperatures from January to April and from August to December, RCA4 (HadGEM2) and CCLM4-8-17 (HadGEM2) replicated the lowest temperatures in this period. The highest air temperatures for each model, average ensemble, and recorded observations were reduced from May to September, reaching the lowest point in July. In contrast, RCA4 (HadGEM2) and CCLM4-8-17 (HadGEM2) displayed a rising pattern with an apex in July. The average monthly and yearly patterns of the highest air temperatures at selected stations across the entire river basin are illustrated in Fig. 3(a–h).

b. Average monthly lowest air temperature pattern

All the models consistently showed a tendency to overestimate the average monthly minimum air temperature, except for the period between February and March, where they underestimated it to varying degrees. The CCLM4-8-17 (HadGEM2) and CCLM4-8-17 (MPI) simulations poorly replicated the minimum air temperature, while the RACMO22T (EC-EARTH) and CanRCM4 (CanESM2) simulations performed better compared to the other models. Most models successfully captured the temperature patterns in the region, except for RCA4 (HadGEM2) and CCLM4-8-17 (HadGEM2), which did not accurately represent them. The models estimated the

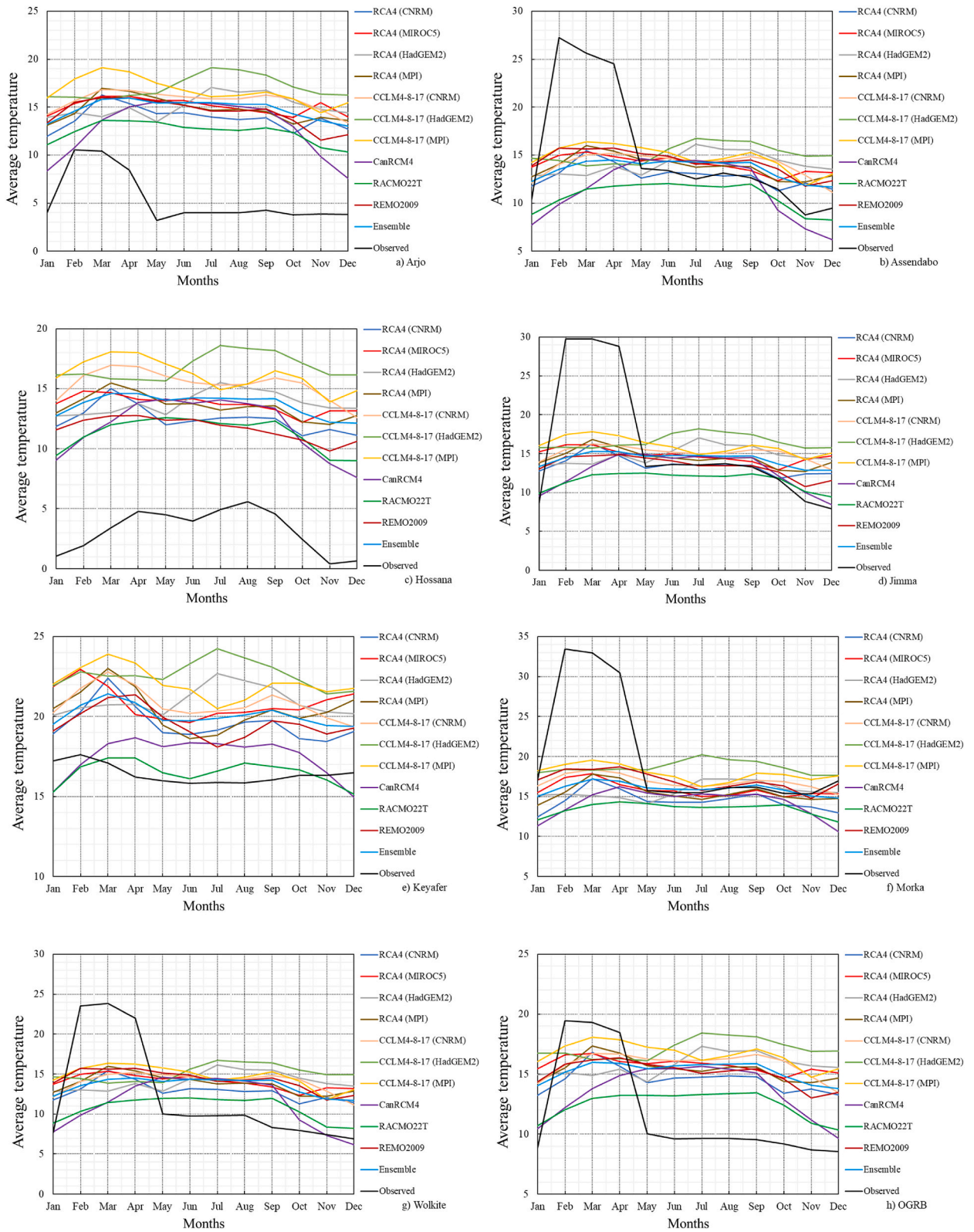


Fig. 4. Average monthly pattern of minimum air temperature for the 10 RCMs, multi-model ensemble (a–g), and observed values for the chosen station and throughout the entire OGRB (h).

Table 2
Coefficient of variation (CV) for the seasonal and annual precipitation and temperature.

Parameters	Seasons	RCA4				CCLM4-8-17				CanRCM4	RACMO22T	REMO2009	Ensemble	Observed
		CNRM	MIROC5	MOHC-Had	MPI	CNRM	MOHC-Had	MPI						
Rainfall	JJAS	7.92	17.19	81	9.04	12.48	54.9	16.29	8.22	10.02	14.17	8.09	14.72	
	MAM	33.9	30.58	116.9	38.14	30.13	104.66	33.77	27.11	23.89	28.69	22.96	24.89	
	Annual	10.18	11.21	24.34	7.9	11.79	20.61	14.07	6.49	7.13	8.2	18.02	9.2	
MaxTMP	JJAS	7.83	6.79	8.09	8.17	7.07	9.07	7.4	7.12	7.18	7.61	7.31	7.24	
	MAM	15.97	15.2	15.9	15.92	15.37	16.65	15.04	15.04	17.25	15.91	15.5	15.49	
	Annual	2.55	3.36	1.78	2.99	4.09	2	4.41	3.74	1.93	3.04	2.5	2.25	
Mini TMP	JJAS	7.44	6.45	7.35	7.95	7.05	7.6	7.45	6.67	7.27	7.68	6.96	11.4	
	MAM	16.42	16	18.18	16.47	15.75	16.24	15.96	16.98	16.51	15.72	16.1	15.47	
	Annual	2.41	3.96	4.21	3.82	1.76	2.12	2.09	4.63	2.37	2.91	1.74	13.91	

highest temperatures from January to April and August to October, with the lowest temperatures gradually increasing from January to May but decreasing from September to October, as depicted in Fig. 4. Fig. 4(a–h) illustrates the patterns of average monthly and yearly minimum air temperature at different stations across the river basin.

The systematic errors in reproducing the highest and lowest annual average air temperatures by the RCA4 (HadGEM2) and CCLM4-8-17 (HadGEM2) climate models can have significant implications for climate impact assessments, especially for sectors sensitive to temperature variations. The obtained results confirmed that when evaluating the impacts of climate change, it is important to consider the accuracy of RCMs. Because of errors in temperature simulations can affect the ability to capture regional differences and the ability to predict and assess the impacts of extreme events, which leads to biased estimates of climate change impacts across various sectors and regions [4,5,66]. For instance, RCMs which consistently underestimate temperature increases over several decades, it may underestimate the cumulative impacts of climate change on ecosystems, human health, and infrastructure [67]. RCMs that consistently underestimate or overestimate temperature increases lead to biased estimates of the impacts of climate change on human health concerning heat stress and air quality, resulting in potentially suboptimal adaptation strategies [67–69]. Similarly, In the agricultural sector, errors in temperature simulations can affect the ability to assess the impacts of climate change on crop yields and water resources. RCMs underestimate temperature increases, and may underestimate the risks of drought and water scarcity [34,70]. Further, in the energy sector, RCMs that underestimate temperature increases can lead to suboptimal energy efficiency and renewable energy strategies, as they may underestimate the risks of increased cooling demand [71,72]. Overall, the systematic errors in reproducing the highest and lowest annual average air temperatures by climate models like RCA4 (HadGEM2) and CCLM4-8-17 (HadGEM2) can hinder climate impact assessments in sectors sensitive to temperature variations. Therefore, it is crucial to carefully evaluate RCMs and only consider the best-performing models in climate change impact assessments.

5.4. Climatic variation in the annual and seasonal time scale

5.4.1. Annual and season-based precipitation variation

The analysis revealed that the yearly and JJAS seasonal precipitation variation had been noticed below 20% for most of the RCMs, excluding RCA4 (HadGEM2) and CCLM4-8-17 (HadGEM2) results, as shown in Table 2. The coefficient of variation for March to May (MAM) precipitation ranged between 20 and 30%, falling into the moderate category, excluding the RCA4 and CCLM4-8-17 RCMs families. Most RCA4 categories, exclusive of RCA4 (MPI), and all CCLM4-8-17 categories overestimated the inter-annual variation of rainfall relatively. The RCA4 (HadGEM2) and CCLM4-8-17 (HadGEM2) models had difficulties in precisely predicting the seasonal fluctuations of JJAS rainfall patterns. Additionally, it was observed that in the March–May periods, the RCMs results produced higher estimates of rainfall discrepancy in the region compared to observations. However, RACMO22T (EC-EARTH), REMO2009 (MPI), CanRCM4 (CanESM2), and ensembles provided more accurate results. The interannual variation in seasonal rainfall anomalies throughout the study area was assessed by applying measured rainfall data, ten RCMs, and an averaged ensemble, as illustrated in Fig. 5.

In general, the reproduced model's rainfall revealed greater fluctuations during the MAM seasons compared to the JJAS season, which suggests the summer seasonal rainfall was relatively stable. Additionally, the mean ensemble values for JJAS and MAM showed less variability in contrast with the corresponding coefficient of variation (CV) estimates observed. The multiple modal ensemble mean data displayed moderate consistency with the measured data during the years analyzed and corresponded with the conclusions drawn by other researchers studying similar phenomena in different geographic regions [4,5,73].

5.4.2. Average annual and seasonal air temperature variations

The result revealed that both the average yearly and seasonal variations in air temperature were within the lower spectrum of variation, with seasonal variations remaining under 20%. In addition, the MAM season experienced higher temperature variability in comparison to the JJAS season, while the maximum air temperatures recorded by the RCMs exhibited marginally greater variation than minimum air temperatures. The interannual temperature variability was observed to be lower in comparison to the seasonal differences found during the JJAS and MAM seasons within the basin, as shown in Table 2.

The climate parameters indicated in Table 2, Max TMP designates Maximum Temperature and Mini TMP designates Minimum Temperature.

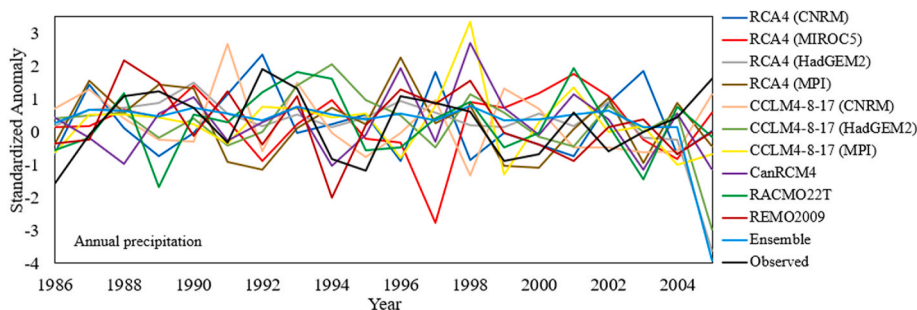


Fig. 5. The interannual variation in annual precipitation anomalies for the observations, the ten RCMs, and their ensemble mean.

Besides, to examine the fluctuations in minimum and maximum air temperatures over time, seasonal anomalies for JJAS) and MAM was considered based on interannual changeability. This anomalies calculation was determined relative to the average minimal and maximal temperatures recorded during the 20 years from 1986 to 2005. The inherent seasonal variation present in simulated and measured values was converted into standardized anomalies. Finally, the minimal and maximal air temperature anomalies for the whole region were standardized using the standard deviation calculated over the two-decade period.

During the periods of 1986–1990 and 1996 to 1998, a negative anomaly in the measured yearly maximal air temperature was produced by most models, as well as the actual measurements. From 1991 to 1995, most RCMs also displayed negative anomalies, although the observed data exhibited a positive anomaly, except in 1993, when a negative anomaly was seen and confirmed with most RCMs output, except for RCA4 (MIROC5). Despite some fluctuation in the observed data, most models successfully reproduced positive anomalies in maximum air temperature between 1999 and 2005. The JJAS and MAM seasonal-based maximal air temperature anomaly indicated a rise in air temperature from 1986 to 2005 for the majority of the models, except a few. However, in 2004 both the observed data and all models displayed negative anomalies. The RCA4 (MIROC5) exhibited considerable changeability related to other models when capturing JJAS, while the CanRCM4 (CanESM2) showed similar variability for MAM seasonal annual maximum air temperature anomalies.

During the periods of 1986, and 1992–1997, the annual minimum air temperature simulations mainly produced negative anomalies, while positive anomalies were observed in 1989–1990, and from 2000 to 2002, and 2004 periods. Slight differences between the simulated and observed minimum air temperatures were noted in 1986, 1994–1988, and 2003, particularly for the JJAS and MAM seasons. Among all RCMs, the minimum air temperature was better simulated during the JJAS season. Seasonal variations showed an increase in minimum air temperature from 1987 to 1992 and 1999–2002 during the spring and summer seasons. Negative anomalies were observed for both JJAS and MAM seasons in all models and observed data between 2004 and 2005. The interannual variation of seasonal lowest air temperature and highest air temperature anomaly for measured temperatures, ten RCMs, and ensembles are depicted in Fig. 6(a–f).

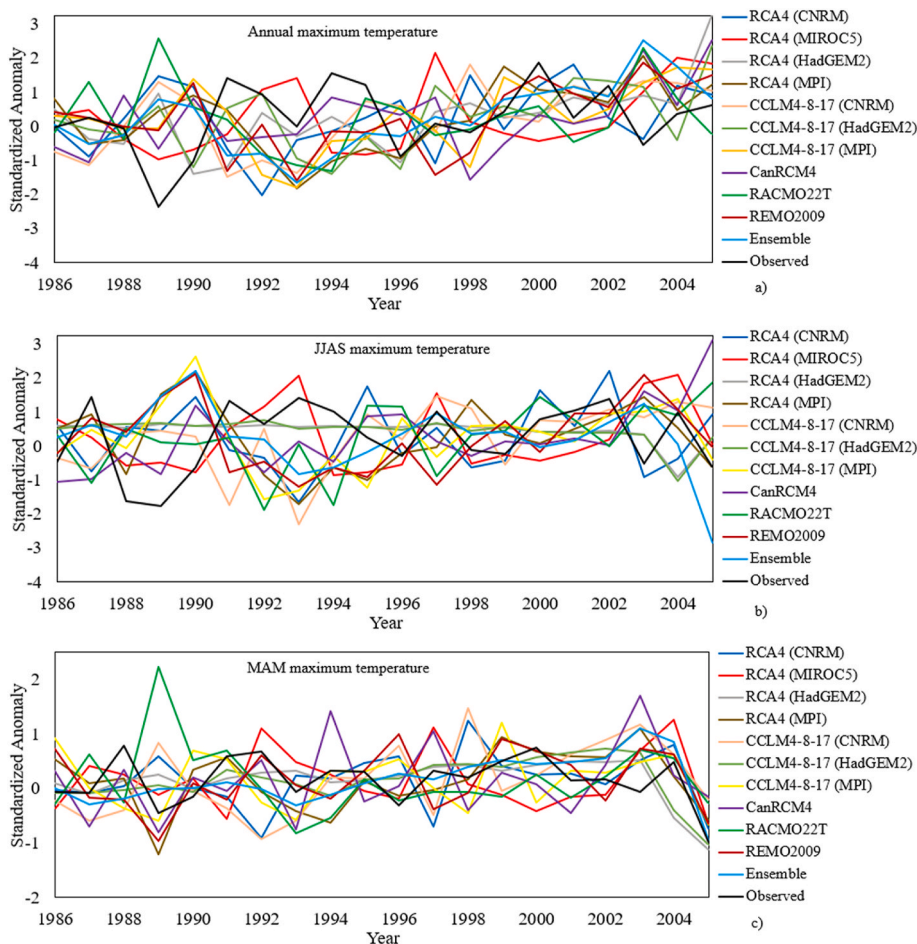


Fig. 6. The interannual variability of seasonal maximum air temperature (a–c) and minimum air temperature (d–f) anomalies.

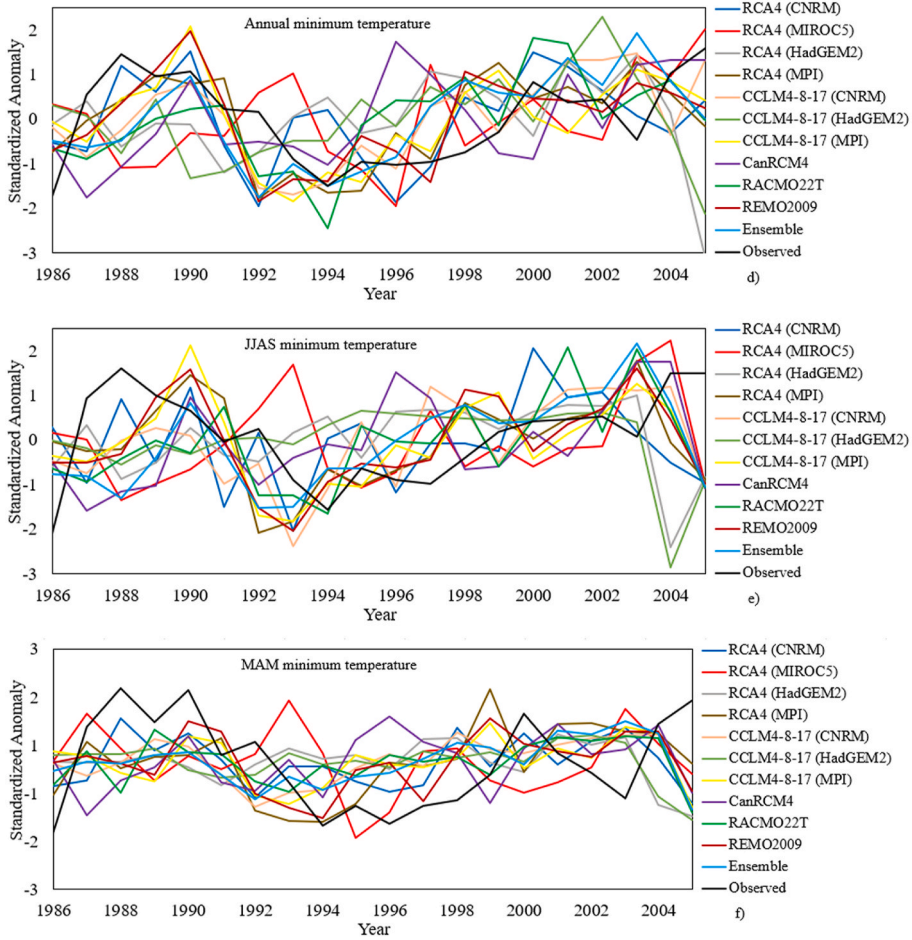


Fig. 6. (continued).

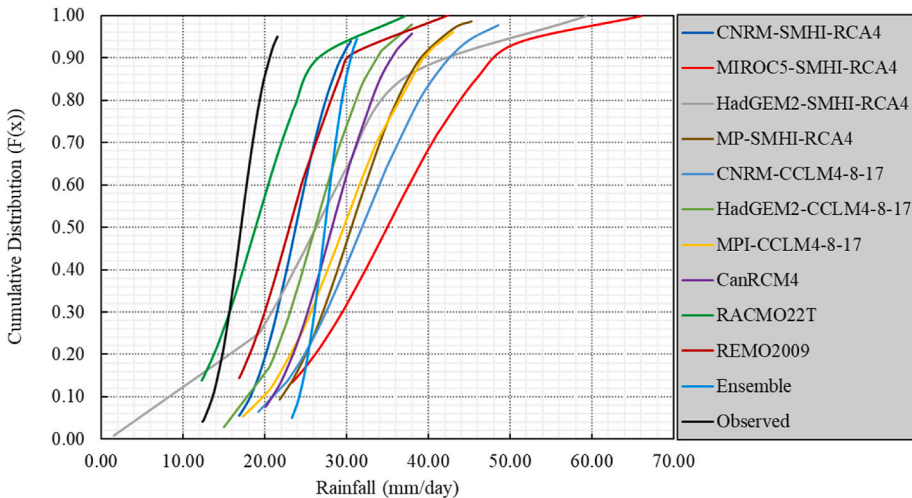


Fig. 7. Comprehensive areal rainfall distribution analysis across the whole OGRB.

5.5. Characteristics of observed precipitation and RCMs

Investigations of the features of excessive precipitation events, and spatial rainfall data were utilized from the entire basin between 1986 and 2005. Observations and simulations from various RCMs with different boundary conditions during the same period revealed notable discrepancies among the models. The maximum extreme value type I cumulative distributions were employed for the analysis. RCA4 (MIROC5) showed a reasonable representation of extreme precipitation distribution when compared to other models (Fig. 7). All models predicted a high likelihood of heavy precipitation, though observational data did not indicate any potential for extreme precipitation events surpassing 21.5 mm/day. Return periods were consistently overestimated by all RCMs, encompassing their average ensemble (Fig. 8). However, the various RCMs ensemble RACMO22T (EC-EARTH) and RCA4 (CNRM) demonstrated better replication of return periods with smaller errors compared to other models. Conversely, RCA4 (MIROC5), CCLM4-8-17 (HadGEM2), and CCLM4-8-17 (CNRM) simulations profoundly overestimate return periods, resulting in the highest errors (Fig. 8). These results were found consistent with those reported by Ref. [4].

5.6. Characterization of spatially averaged annual precipitation

In the considered region, the complex topography of the expanse causes significant variations in precipitation amounts and spatial distribution. The spatial distribution of precipitation throughout the basin was scrutinized employing the RCMs and measured precipitation records between 1986 and 2005, as shown in Fig. 9. The results showed that the average yearly minimum precipitation was 0.27 mm and 0.49 mm at Dimeka and Jinka stations, as per the CCLM4-8-17 (HadGEM2) model, while the RCA4 group of regional climate models predicted the highest yearly average rainfall between 7.5 mm and 10.4 mm in the Emdibir and Hosana stations. The various model ensembles generated the highest annual average precipitations of 5.74 mm in the Emdibir, while the lowest value of 1.47 mm at the Wolaita Sodo observations. The CCLM4-8-17 RCMs of all groups and REMO2009 (MPI) effectively mimic the highest annual average precipitation at Woliso and the lowest at Dimeka, excluding CCLM4-8-17 (CNRM) which reproduced the smallest amount of rainfall at Wolaita Sodo observation. Conversely, the climate models CanRCM4 (CanESM2) and RACMO22T (EC-EARTH) successfully captured maximum precipitation at Bonga and Bako, while a minimum is observed at the Wolaita Sodo observation. The analysis of the observational data revealed significant variations in average annual precipitation across different locations. Dedo station recorded the highest value of 5.27 mm, while Limu-Genet station experienced a slightly lower value of 4.89 mm. On the other hand, Gojeb and Dimeka stations reported significantly lower precipitation rates of 0.94 mm and 1.65 mm respectively, as illustrated in Fig. 9. The upper reaches of the basin experienced higher average annual maximum precipitation in contrast to the lower areas of the basin. Most RCM simulations and the average ensemble predicted low rainfall values in the basin’s lower areas and moderate rainfall in the central parts. In comparison, the ensemble means and RACMO22T (EC-EARTH) demonstrated greater in simulating the average annual rainfall spatial occurrence. Fig. 9(a–l) illustrates the spatial average yearly rainfall distribution between 1986 and 2005 for observations, ten RCMs, and their average ensemble across the basin. The findings of this study corroborate the differences among the various models employed in depicting climatic phenomena both in space and time, which was found consistent with earlier investigations carried out in varied areas of the country [4,5,19].

Overall, the spatiotemporal differences in the amount of rainfall in the OGRB can have significant consequences for agriculture and water management. The implications include the possibility of water scarcity in areas that are already experiencing water stress and an increase in water variability and uncertainty. These differences in rainfall could lead to a reduction in the availability of water for irrigation, domestic use, hydropower production, and other purposes, which could negatively affect crop yields, food security, and the livelihoods of local communities. Therefore, to adapt to changing climate conditions, proactive measures such as adopting drought-resistant crops, conservation practices, and efficient irrigation techniques, and implementing effective water allocation, and land

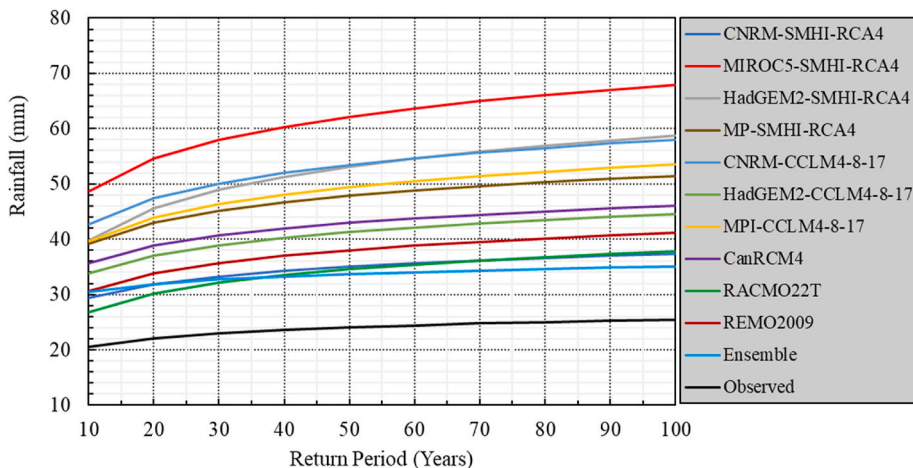


Fig. 8. Analysis of the annually-occurring maximum areal rainfall events and their respective return periods within the OGRB.

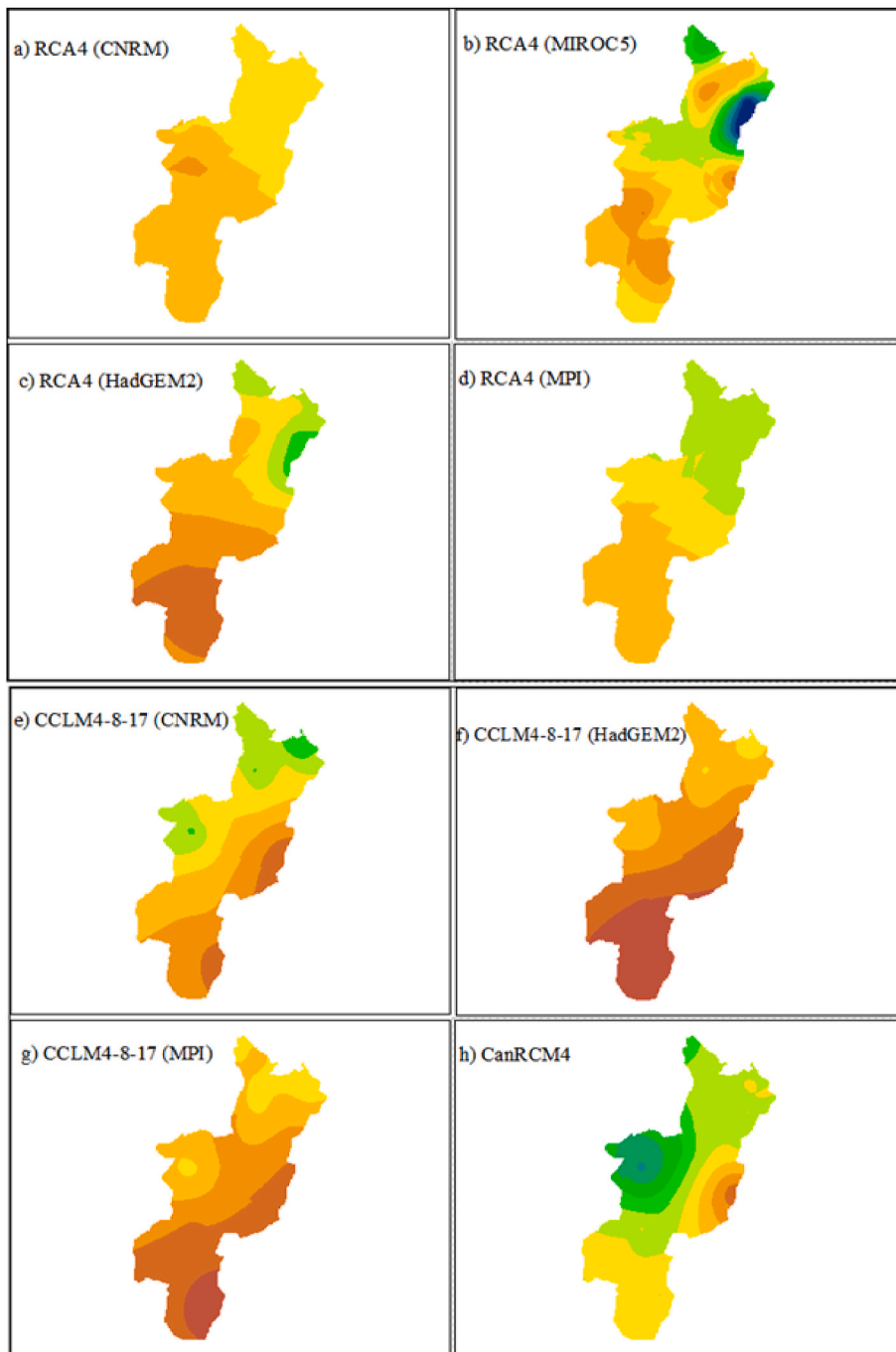


Fig. 9. Spatial distribution of average yearly precipitation from ten RCMS, ensemble (a-k), and observed data (l) from 1986 to 2005 in the OGRB.

and water resources management policies are necessary.

6. Conclusions

The performance of RCMs in replicating the spatial patterns of precipitation and air temperature has varied across regions and models, posing a challenge to the verification and application of their outputs. To that end, this study aimed to determine the CORDEX Africa RCM's ability to reproduce precipitation and air temperature by comparing it with observed data from 1986 to 2005. The RCM's

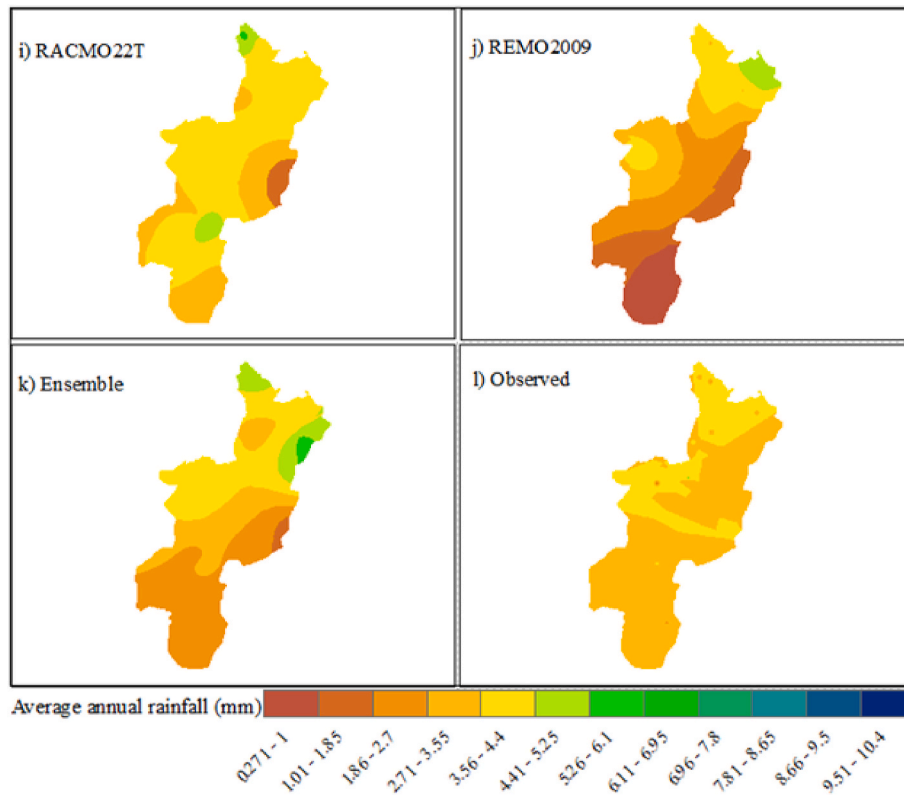


Fig. 9. (continued).

performance varied at both space and time and was superior in capturing precipitation during dry months than wet months. However, some models struggled to capture the quantity and climatic conditions of rainfall across the entire area. Most models overestimated precipitation during wet months, while RCA4 (HadGEM2), CCLM4-8-17 (CNRM), CCLM4-8-17 (HadGEM2), and CCLM4-8-17 (MPI) underestimate it. The multi-model ensemble data provided a better agreement with observations than individual RCMs in precipitation and air temperature simulations. Interannual and seasonal variations were observed in the lowest categories for both precipitation and air temperature. All RCMs overestimated areal precipitation extremes and return periods, and they were better at replicating maximum air temperatures than minimums. Some models over-simulated the yearly average minimum air temperature, while others under-simulated the yearly average maximal temperature. The RACMO22T (EC-EARTH) model performed best in simulating the minimal air temperature, whereas the RACMO22T (EC-EARTH) and CCLM4-8-17 (CNRM) models performed poorly at determining the maximal annual average air temperature. The best-performing RCMs included RACMO22T (EC-EARTH), CCLM4-8-17 (CNRM), RCA4 (CNRM), CCLM4-8-17 (MPI), REMO2009 (MPI), and RCA4 (MPI), while the RCA4 (HadGEM2) and CCLM4-8-17 (HadGEM2) outcomes captured poorly in reproducing the OGRB climatic conditions. In general, the evaluation of the CORDEX-Africa regional climate models demonstrated their importance for analyzing climate change effects in Eastern Africa, mainly in the OGRB, Ethiopia. However, the study also revealed consistent deviations in model performance, indicating the necessity of using a multi-model ensemble approach after conducting a careful evaluation of RCM outputs against observed datasets. This further highlights the need for bias adjustments in RCM simulations and conducting sensitivity analyses at various spatial resolutions before applying these simulations for decision-making and environmental impact studies. Additionally, for future investigations, it is recommended to explore the influence of different resolutions, including finer scales, on model performance and regional climate representation. This could involve integrating hydrological models to assess the implications of simulated climate variables on the hydrological regime. Moreover, incorporating socio-economic data and engaging stakeholders would be valuable in assessing the vulnerability and resilience of communities in the OGRB to evolving climate conditions, thus informing appropriate adaptation strategies.

Author contribution statement

Yonas Mathewos, Brook Abate, Mulugeta Dadi: Conceived and designed the experiments; Performed the experiments; Analyzed and interpreted the data; Contributed reagents, materials, analysis tools or data; Wrote the paper.

Data availability statement

Data included in article/supplementary material/referenced in article.

Funding statement

This research did not receive any specific grant from funding agencies in the public, commercial, or not-for-profit sectors.

Declaration of competing interest

The authors declare that they have no known competing financial interests or personal relationships that could have appeared to influence the work reported in this paper.

Acknowledgments

We would like to express our deepest gratitude to the Hawassa University Institute of Technology for their support in conducting this research. We thank the global Earth System Grid Federation for providing the CORDEX data and the National Meteorological Service Agency of Ethiopia for providing the observed station data. We also extend our heartfelt appreciation to the reviewers and editors of the Journal of Heliyon, whose valuable feedback and suggestions have played an instrumental role in refining our manuscript.

Appendix A. Supplementary data

Supplementary data related to this article can be found at <https://doi.org/10.1016/j.heliyon.2023.e20379>.

References

- [1] C. Frei, R. Schöll, S. Fukutome, J. Schmidli, P.L. Vidale, Future change of precipitation extremes in Europe: intercomparison of scenarios from regional climate models, *J. Geophys. Res. Atmos.* 111 (2006), <https://doi.org/10.1029/2005JD005965>.
- [2] J.L. Bell, L.C. Sloan, M.A. Snyder, Regional changes in extreme climatic events: a future climate scenario, *J. Clim.* 17 (2004) 81–87.
- [3] A. Asfaw, A. Bantider, B. Simane, A. Hassen, Smallholder farmers' livelihood vulnerability to climate change-induced hazards: agroecology-based comparative analysis in Northcentral Ethiopia (Woleka Sub-basin), *Heliyon* 7 (2021), e06761.
- [4] T.A. Demissie, C.H. Sime, Assessment of the performance of CORDEX regional climate models in simulating rainfall and air temperature over southwest Ethiopia, *Heliyon* 7 (2021), e07791, <https://doi.org/10.1016/j.heliyon.2021.e07791>.
- [5] W.T. Dibaba, K. Miegel, T.A. Demissie, Evaluation of the CORDEX regional climate models performance in simulating climate conditions of two catchments in Upper Blue Nile Basin, *Dynam. Atmos. Oceans* 87 (2019), 101104.
- [6] C. Ofoegbu, P.W. Chirwa, J. Francis, F.D. Babalola, Assessing local-level forest use and management capacity as a climate-change adaptation strategy in Vhembe district of South Africa, *Clim. Dev.* 11 (2019) 501–512.
- [7] E.A. Warnatzsch, D.S. Reay, Temperature and precipitation change in Malawi: evaluation of CORDEX-Africa climate simulations for climate change impact assessments and adaptation planning, *Sci. Total Environ.* 654 (2019) 378–392, <https://doi.org/10.1016/j.scitotenv.2018.11.098>.
- [8] K.I. Adenuga, A.S. Mahmoud, Y.A. Dodo, M. Albert, S.A. Kori, N.J. Danlami, Climate change adaptation and mitigation in sub-saharan African countries, *Energy and Environmental Security in Developing Countries* (2021) 393–409.
- [9] B. Ayugi, H.N. Nadoya, H. Babausmail, R. Karim, V. Iyakaremye, K. Lim Kam Sian, V. Ongoma, Evaluation and projection of mean surface temperature using CMIP6 models over East Africa, *J. Afr. Earth Sci.* (2021), <https://doi.org/10.1016/j.jafrearsci.2021.104226>.
- [10] G. Yigezu, The challenges and prospects of Ethiopian agriculture, *Cogent Food Agric.* 7 (2021), 1923619, <https://doi.org/10.1080/23311932.2021.1923619>.
- [11] D. Welteji, A critical review of rural development policy of Ethiopia: access, utilization and coverage, *Agric. Food Secur.* 7 (2018) 55, <https://doi.org/10.1186/s40066-018-0208-y>.
- [12] S. Asseng, F. Ewert, P. Martre, R.P. Rötter, D.B. Lobell, D. Cammarano, B.A. Kimball, M.J. Ottman, G.W. Wall, J.W. White, Rising temperatures reduce global wheat production, *Nat. Clim. Change* 5 (2015) 143–147.
- [13] S.H. Gebrechorkos, S. Hülsmann, C. Bernhofer, Changes in temperature and precipitation extremes in Ethiopia, Kenya, and Tanzania, *Int. J. Climatol.* 39 (2019) 18–30.
- [14] F.A. Anose, K.T. Beketie, T.T. Zeleke, D.Y. Ayal, G.L. Feyisa, B.T. Haile, Spatiotemporal analysis of droughts characteristics and drivers in the Omo-Gibe River basin, Ethiopia, *Environmental Systems Research* 11 (2022) 3, <https://doi.org/10.1186/s40068-022-00246-8>.
- [15] A. Teshome, J. Zhang, Increase of extreme drought over Ethiopia under climate warming, *Adv. Meteorol.* (2019) 2019.
- [16] D.-L. Guo, J.-Q. Sun, E.-T. Yu, Evaluation of CORDEX regional climate models in simulating temperature and precipitation over the Tibetan Plateau, *Atmospheric and Oceanic Science Letters* 11 (2018) 219–227, <https://doi.org/10.1080/16742834.2018.1451725>.
- [17] G. Pang, X. Wang, D. Chen, M. Yang, L. Liu, Evaluation of a climate simulation over the Yellow River Basin based on a regional climate model (REMO) within the CORDEX, *Atmos. Res.* 254 (2021), 105522.
- [18] S. Stefanidis, S. Dafis, D. Stathis, Evaluation of regional climate models (RCMs) performance in simulating seasonal precipitation over Mountainous Central Pindus (Greece), *Water* 12 (2020) 2750.
- [19] R. Girma, C. Fürst, A. Moges, Performance evaluation of CORDEX-Africa regional climate models in simulating climate variables over Ethiopian main rift valley: evidence from Gidabo river basin for impact modeling studies, *Dynam. Atmos. Oceans* 99 (2022), 101317.
- [20] G. Worku, E. Teferi, A. Bantider, Y.T. Dile, M.T. Taye, Evaluation of regional climate models performance in simulating rainfall climatology of Jemma sub-basin, Upper Blue Nile Basin, Ethiopia, *Dynam. Atmos. Oceans* 83 (2018) 53–63.
- [21] E. Pastén-Zapata, J.M. Jones, H. Moggridge, M. Widmann, Evaluation of the performance of Euro-CORDEX Regional Climate Models for assessing hydrological climate change impacts in Great Britain: a comparison of different spatial resolutions and quantile mapping bias correction methods, *J. Hydrol.* 584 (2020), 124653, <https://doi.org/10.1016/j.jhydrol.2020.124653>.

- [22] A.A. Akinsanola, K.O. Ogunjobi, I.E. Gbode, V.O. Ajayi, Assessing the capabilities of three regional climate models over CORDEX Africa in simulating west african summer monsoon precipitation, *Advances in Meteorology*. 2015 (2015), e935431, <https://doi.org/10.1155/2015/935431>.
- [23] A. Dosio, H.-J. Panitz, M. Schubert-Frisius, D. Lüthi, Dynamical downscaling of CMIP5 global circulation models over CORDEX-Africa with COSMO-CLM: evaluation over the present climate and analysis of the added value, *Clim. Dynam.* 44 (2015) 2637–2661.
- [24] P. Luhunga, J. Botai, F. Kahimba, Evaluation of the performance of CORDEX regional climate models in simulating present climate conditions of Tanzania, *JSHES 66* (2016) 32–54, <https://doi.org/10.1071/es16005>.
- [25] E. Mutayoba, J.J. Kashaigili, Evaluation for the Performance of the CORDEX Regional Climate Models in Simulating Rainfall Characteristics over Mbarali River Catchment in the Rufiji Basin, Tanzania, 2017.
- [26] H.S. Endris, C. Lennard, B. Hewitson, A. Dosio, G. Nikulin, H.-J. Panitz, Teleconnection responses in multi-GCM driven CORDEX RCMs over Eastern Africa, *Clim. Dynam.* 46 (2016) 2821–2846, <https://doi.org/10.1007/s00382-015-2734-7>.
- [27] D. Etana, C.F. van Wesenbeeck, T. de Cock Buning, Socio-cultural aspects of farmers' perception of the risk of climate change and variability in Central Ethiopia, *Clim. Dev.* 13 (2021) 139–151.
- [28] W.G. Namara, G.M. Hirpo, T.A. Feyissa, Evaluation of impact of climate change on the watershed hydrology, case of Wabe Watershed, Omo Gibe River basin, Ethiopia, *Arabian J. Geosci.* 15 (2022) 1356, <https://doi.org/10.1007/s12517-022-10585-6>.
- [29] Z.A. Tilahun, Y.K. Bizuneh, A.G. Mekonnen, The impacts of climate change on hydrological processes of Gilgel Gibe catchment, southwest Ethiopia, *PLoS One* 18 (2023), <https://doi.org/10.1371/journal.pone.0287314>.
- [30] M. Toma, M. Belete, M. Ulsido, Hydrological components and sediment yield response to land use land cover change in the ajora-woybo watershed of omo-gibe basin, Ethiopia, *Air Soil. Water Res.* 16 (2023) 1–17, <https://doi.org/10.1177/11786221221150186>.
- [31] Y. Abose, T. Begeho, Evaluations of Stream Flow Response to Land Use and Land Cover Changes in Wabe Watershed, Omo-Gibe Basin, Ethiopia, *Civil and Environmental Research*, 2020, <https://doi.org/10.7176/CER/12-10-02>.
- [32] S.E. Chaemiso, S.A. Kartha, S.M. Pingale, Effect of land use/land cover changes on surface water availability in the Omo-Gibe basin, Ethiopia, *Hydrol. Sci. J.* 66 (2021) 1936–1962.
- [33] H. Daniel, Hydrological response to climate change in the Deme watershed, Omo-Gibe Basin, Ethiopia, *Journal of Water and Climate Change* 14 (2023) 1112–1131, <https://doi.org/10.2166/wcc.2023.248>.
- [34] T.P. Orkojdo, G. Kranjac-Berisavijevic, F.K. Abagale, Impact of climate change on future availability of water for irrigation and hydropower generation in the Omo-Gibe Basin of Ethiopia, *J. Hydrol.: Reg. Stud.* 44 (2022), 101254, <https://doi.org/10.1016/j.ejrh.2022.101254>.
- [35] W. Abebe, Evaluation of groundwater resource potential by using water balance model: a case of Upper Gilgel Gibe Watershed, Ethiopia 10 (2022) 209–222, <https://doi.org/10.19637/j.cnki.2305-7068.2022.03.001>.
- [36] T.D. Mengistu, I.-M. Chung, M.-G. Kim, S.W. Chang, J.E. Lee, Impacts and implications of land use land cover dynamics on groundwater recharge and surface runoff in East African watershed, *Water* 14 (2022) 2068, <https://doi.org/10.3390/w14132068>.
- [37] M.A. Degefu, W. Bewket, Variability and trends in rainfall amount and extreme event indices in the Omo-Ghibe River Basin, Ethiopia, *Reg. Environ. Change* 14 (2014) 799–810, <https://doi.org/10.1007/s10113-013-0538-z>.
- [38] M. Werner Worku, N. Wright, P. van der Zaag, S.S. Demissie, Flow regime change in an endorheic basin in southern Ethiopia, *Hydrol. Earth Syst. Sci.* 18 (2014) 3837–3853, <https://doi.org/10.5194/hess-18-3837-2014>.
- [39] G. Nikulin, C. Jones, F. Giorgi, G. Arsar, M. Büchner, R. Cerezo-Mota, O.B. Christensen, M. Déqué, J. Fernandez, A. Hänsler, E. van Meijgaard, P. Samuelsson, M. B. Sylla, L. Sushama, Precipitation climatology in an ensemble of CORDEX-africa regional climate simulations, *J. Clim.* 25 (2012) 6057–6078, <https://doi.org/10.1175/JCLI-D-11-00375.1>.
- [40] K.E. Taylor, R.J. Stouffer, G.A. Meehl, An overview of CMIP5 and the experiment design, *Bull. Am. Meteorol. Soc.* 93 (2012) 485–498.
- [41] S.M. Yimer, A. Bouanani, N. Kumar, B. Tischbein, C. Borgemeister, Assessment of climate models performance and associated uncertainties in rainfall projection from CORDEX over the eastern Nile basin, Ethiopia, *Climatic Change* 10 (2022) 95, <https://doi.org/10.3390/cli10070095>.
- [42] C. Yoo, E. Cho, Comparison of GCM precipitation predictions with their RMSEs and pattern correlation coefficients, *Water* 10 (2018) 28, <https://doi.org/10.3390/w10010028>.
- [43] E. van Meijgaard, L.H. Van Ulft, W.J. Van de Berg, F.C. Bosveld, B. Van den Hurk, G. Lenderink, A.P. Siebesma, The KNMI Regional Atmospheric Climate Model RACMO, KNMI De Bilt, The Netherlands, 2008 version 2.1.
- [44] P. Samuelsson, C.G. Jones, U. Willm' En, A. Ullerstig, S. Gollvik, U.L.F. Hansson, E. Jansson, C. Kjellstro, M.G. Nikulin, K. Wyser, The Rossby Centre Regional Climate model RCA3: model description and performance, *Tellus Dyn. Meteorol. Oceanogr.* 63 (2011) 4–23.
- [45] V. Platonov, A. Kislov, High-resolution COSMO-CLM modeling and an assessment of mesoscale features caused by coastal parameters at near-shore arctic zones (kara sea), *Atmosphere* 11 (2020) 1062, <https://doi.org/10.3390/atmos11101062>.
- [46] D. Jacob, L. Bärring, O.B. Christensen, J.H. Christensen, M. de Castro, M. Déqué, F. Giorgi, S. Hagemann, M. Hirschi, R. Jones, An inter-comparison of regional climate models for Europe: model performance in present-day climate, *Climatic Change* 81 (2007) 31–52.
- [47] D. Caya, R. Laprise, M. Giguère, G. Bergeron, J.P. Blanchet, B.J. Stocks, G.J. Boer, N.A. McFarlane, Description of the Canadian regional climate model, *Water Air Soil Pollut.* 82 (1995) 477–482.
- [48] A. Zadra, D. Caya, J. Côté, B. Dugas, C. Jones, R. Laprise, K. Winger, L.-P. Caron, The next Canadian regional climate model, *Phys. Can.* 64 (2008) 75–83.
- [49] G.T. Diro, T. Toniazzo, L. Shaffrey, Ethiopian rainfall in climate models, in: *African Climate and Climate Change*, Springer, 2011, pp. 51–69.
- [50] N.P. Vidal, C.F. Manful, T.H. Pham, P. Stewart, D. Keough, R. Thomas, The use of XLSTAT in conducting principal component analysis (PCA) when evaluating the relationships between sensory and quality attributes in grilled foods, *MethodsX* 7 (2020), 100835.
- [51] I. Ahmad, T. Ahmad, M. Ibrahim, Modelling of Extreme Rainfall in Punjab: Pakistan Using Bayesian and Frequentist Approach, vol. 17, *Applied Ecology & Environmental Research*, 2019.
- [52] T. Ahmad, I. Ahmad, I.A. Arshad, N. Bianco, A comprehensive study on the Bayesian modelling of extreme rainfall: a case study from Pakistan, *Int. J. Climatol.* 42 (2022) 208–224.
- [53] O. Agha, S.Ç. Bağçacı, N. Şarлак, Homogeneity analysis of precipitation series in North Iraq, *IOSR J. Appl. Geol. Geophys.* 5 (2017) 57–63.
- [54] R. Elzeiny, M. Khadr, S. Zahran, E. Rashwan, Homogeneity analysis of rainfall series in the upper blue Nile river basin, Ethiopia, *Journal of Engineering Research* 3 (2019) 46–53.
- [55] A. Martynov, R. Laprise, L. Sushama, K. Winger, L. Šeparović, B. Dugas, Reanalysis-driven climate simulation over CORDEX North America domain using the Canadian Regional Climate Model, version 5: model performance evaluation, *Clim. Dynam.* 41 (2013) 2973–3005.
- [56] M. Mendez, B. Maathuis, D. Hein-Griggs, L.-F. Alvarado-Gamboa, Performance evaluation of bias correction methods for climate change monthly precipitation projections over Costa Rica, *Water* 12 (2020) 482.
- [57] V. Ongoma, H. Chen, C. Gao, Evaluation of CMIP5 twentieth century rainfall simulation over the equatorial East Africa, *Theor. Appl. Climatol.* 135 (2019) 893–910.
- [58] Y. Bayissa, T. Tadesse, G. Demisse, A. Shiferaw, Evaluation of satellite-based rainfall estimates and application to monitor meteorological drought for the Upper Blue Nile Basin, Ethiopia, *Rem. Sens.* 9 (2017) 669.
- [59] E.P. Diaconescu, P. Gachon, R. Laprise, J.F. Scinocca, Evaluation of precipitation indices over North America from various configurations of regional climate models, *Atmos.-Ocean* 54 (2016) 418–439.
- [60] A. Shiferaw, T. Tadesse, C. Rowe, R. Oglesby, Precipitation extremes in dynamically downscaled climate scenarios over the Greater Horn of Africa, *Atmosphere* 9 (2018) 112.
- [61] A.A. Mekonen, A.B. Berlie, Spatiotemporal variability and trends of rainfall and temperature in the Northeastern Highlands of Ethiopia, *Modeling Earth Systems and Environment* 6 (2020) 285–300.
- [62] S. Ly, C. Charles, A. Degre, Geostatistical interpolation of daily rainfall at catchment scale: the use of several variogram models in the Ourthe and Ambleve catchments, Belgium, *Hydrol. Earth Syst. Sci.* 15 (2011) 2259–2274.

- [63] Y. Jambo, A. Alemu, W. Tasew, Impact of small-scale irrigation on household food security: evidence from Ethiopia, *Agric. Food Secur.* 10 (2021) 21, <https://doi.org/10.1186/s40066-021-00294-w>.
- [64] R. Solomon, B. Simane, B.F. Zaitchik, The impact of climate change on agriculture production in Ethiopia: application of a dynamic computable general equilibrium model, *Am. J. Clim. Change* 10 (2021) 32–50, <https://doi.org/10.4236/ajcc.2021.101003>.
- [65] S. Swain, A.K. Taloor, L. Dhal, S. Sahoo, N. Al-Ansari, Impact of climate change on groundwater hydrology: a comprehensive review and current status of the Indian hydrogeology, *Appl. Water Sci.* 12 (2022) 120, <https://doi.org/10.1007/s13201-022-01652-0>.
- [66] M. Luo, T. Liu, F. Meng, Y. Duan, A. Frankl, A. Bao, P. De Maeyer, Comparing bias correction methods used in downscaling precipitation and temperature from regional climate models: a case study from the kaidu River Basin in western China, *Water* 10 (2018) 1046, <https://doi.org/10.3390/w10081046>.
- [67] A. Ipc, *IPCC Fifth Assessment Report—Synthesis Report, 2014*.
- [68] D.W. Abel, T. Holloway, M. Harkey, P. Meier, D. Ahl, V.S. Limaye, J.A. Patz, Air-quality-related health impacts from climate change and from adaptation of cooling demand for buildings in the eastern United States: an interdisciplinary modeling study, *PLoS Med.* 15 (2018), e1002599, <https://doi.org/10.1371/journal.pmed.1002599>.
- [69] E.P. Petkova, H. Morita, P.L. Kinney, Health impacts of heat in a changing climate: how can emerging science inform urban adaptation planning? *Curr Epidemiol Rep* 1 (2014) 67–74, <https://doi.org/10.1007/s40471-014-0009-1>.
- [70] C. Sun, X. Zhou, Characterizing hydrological drought and water scarcity changes in the future: a case study in the jinghe River Basin of China, *Water* 12 (2020) 1605, <https://doi.org/10.3390/w12061605>.
- [71] S. Chandramowli, F. Felder, Impact of Climate Change on Electricity Systems and Markets - A Review of Models and Forecasts, *Sustainable Energy Technologies and Assessments*, vol. 5, 2013, <https://doi.org/10.2139/ssrn.2251167>.
- [72] K. Solaun, E. Cerdá, Climate change impacts on renewable energy generation. A review of quantitative projections, *Renew. Sustain. Energy Rev.* 116 (2019), 109415, <https://doi.org/10.1016/j.rser.2019.109415>.
- [73] T. Gadissa, M. Nyadawa, F. Behulu, B. Mutua, The effect of climate change on loss of lake volume: case of sedimentation in central rift valley basin, *Ethiopia, Hydrology* 5 (2018) 67.